Immunity, Vol. 22, 59–70, January, 2005, Copyright ©2005 by Elsevier Inc. DOI 10.1016/j.immuni.2004.11.011

The KSHV Immediate-Early Transcription Factor RTA Encodes Ubiquitin E3 Ligase Activity that Targets IRF7 for Proteosome-Mediated Degradation

Yanxing Yu, Shizhen Emily Wang, and Gary S. Hayward*
Molecular Virology Laboratories
Viral Oncology Program
The Sidney Kimmel Comprehensive Cancer Center
Bunting-Blaustein Cancer Research Building
Johns Hopkins University School of Medicine
1650 Orleans Street
Baltimore, Maryland 21231

Summary

Many viruses encode proteins that counteract the development of the interferon (IFN)-mediated antiviral state. Here, we report that interferon regulatory factor 7 (IRF7), a key mediator of type I IFN induction, is targeted for degradation by binding to the RTA immediate-early nuclear transcription factor encoded by Kaposi's sarcoma-associated herpesvirus (KSHV or HHV8). Cotransfection with RTA blocked IRF7-mediated IFNα and IFNβ mRNA production and promoted the ubiquitination and degradation of IRF7 protein in a proteasome-dependent fashion. Addition of RTA also promoted polyubiquitination of IRF7 in an in vitro cell free assay, demonstrating that RTA itself acts as a ubiquitin E3 ligase. RTA also autoregulated its own polyubiquitination and stability, and both activities were abolished by point mutations in a Cys plus His-rich N-terminal domain. Therefore, manipulation of the stability and function of IRF7 by the KSHV RTA transcription factor provides an unexpected regulatory strategy for circumventing the innate immune defence system.

Introduction

Interferon regulatory factors (IRFs) play critical roles in modulation of the activity of the innate immune system. In particular, IRF3 and IRF7 are specific transcription factors that play pivotal roles in virus-induced IFNα and IFNβ production that is central for the expression of IFN-stimulated genes (ISG) (Mamane et al., 1999; Marie et al., 1998; Sato et al., 2000; Taniguchi et al., 2001). IRFs can also modulate cell growth and differentiation as well as apoptosis.

Although both are essential and bind to similar ISRE-like motifs in ISG target promoters, IRF3 and IRF7 have distinctive roles as conditional nuclear DNA binding proteins in the induction of IFNα/β genes and in establishment of the antiviral state. For example, the induction of IFNα/β promoters is nearly completely abolished in IRF3 and IRF7 null cells, and both are required to restore IFN responses in double knockout DKO cells (Sato et al., 2000). IRF7 is a short half-lived protein that is usually expressed at very low levels, but its expression is highly inducible by IFN, LPS, TPA, and RNA or DNA virus infection. In contrast, IRF3 is often expressed constitutively and appears to be the major player in the early phase of IFN induction. However, in the later or amplification phase of IFN induction, IRF7 is more critical, and its expression becomes higher than that of IRF3. IFNα, NDV, and STAT proteins induce the expression of IRF7 mRNA, whereas Sendai virus, DNA damage, and the EBV latency protein LMP1 increase IRF7 protein levels (Lin et al., 2000; Zhang and Pagano, 2002). Functional activation of both IRF3 and IRF7 includes processes that enhance phosphorylation, dimerization, and nuclear translocation (Au et al., 1998; Lin et al., 1998; Yoneyama et al., 1998).

Despite the importance of IRF7 for defense mechanisms against virus infection, little is known about its physiological regulation at the protein level. IRF7 has a shorter half-life than IRF3 (Sato et al., 2000), and the normally low steady-state levels of IRF7 suggest that IRF7 could be regulated by the ubiquitin (Ub)-proteasome system. A number of other short-lived transcription factors such as P53, c-JUN, c-FOS, STAT1, c-MYC, and E2F are all substrates for the Ub-proteasome pathway (Kubbutat et al., 1997) in which covalent attachment of polyUb chains by the sequential action of Ub-activating enzyme (E1), Ub-conjugating enzyme (E2), and a specific Ub ligase (E3) results in specific targeting to the 26 S proteasome for degradation (Hershko and Ciechanover, 1998; Pickart, 2000).

Many mechanisms for induction of IFN-mediated antiviral responses by RNA viruses have been described, but less is known for most DNA viruses, where the processes involved in both generating and overcoming an antiviral response are often complex and multifactorial. Major strategies for blocking type-1 IFN production include targeting and inhibiting the activities of either the IRF3 or STAT transcription factors (Foy et al., 2003; Goodbourn et al., 2000). Herpesviruses are all thought to induce antiviral responses upon contact with the cell surface, but these effects are later ablated by viral immediate-early lytic cycle gene products (Mossman et al., 2001). For example, gene array studies in cells infected with both HCMV (Zhu et al., 1997) and KSHV (Poole et al., 2002) have detected transcriptional stimulation of virtually all cellular ISGs, including IRF7 mRNA, but not the IFN mRNAs themselves.

KSHV is a DNA tumor virus of the rhadinovirus subfamily that causes rare endothelial and lymphoid tumors and was first discovered in Kaposi's sarcoma (KS) in 1994 (Chang et al., 1994). The rates of KS disease are greatly increased by immunosuppression in both organ transplant patients and AIDS patients. The KSHV-encoded immediate-early RTA protein studied here is a DNA binding nuclear transcription factor that can act as the trigger for the entire KSHV lytic cycle (Sun et al., 1998). RTA targets downstream viral promoters through both direct DNA binding and by formation of protein complexes with at least two cellular DNA binding transcription factors, CBF1 (Liang et al., 2002) and C/EBPα (Wang et al., 2003).

In this report, we demonstrate that IRF7 is regulated

*Correspondence: ghayward@jhmi.edu

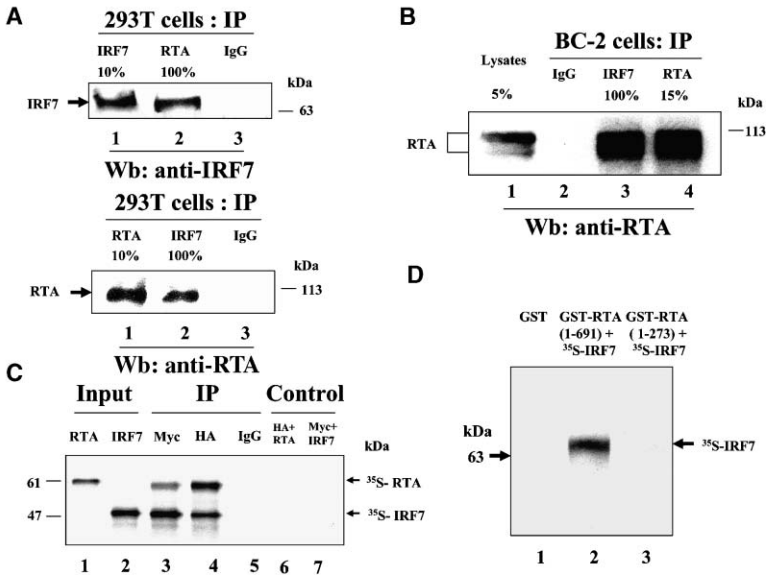

Figure 1. Detection of Physical Interactions between the RTA and IRF7 Proteins Both Intracellularly and In Vitro

(A) The intact RTA(1–691) and FLAG-IRF7 (1–503) expression plasmids were cotransfected at a 3 μg to 10 μg ratio into 293T cells. The proteins were immunoprecipitated from whole-cell extracts (WCE) with either anti-IRF7 PAb, anti-RTA Pab, or with a nonspecific control antibody (IgG) as indicated then immunoblotted (Wb) with either the anti-IRF7 (top) or anti-RTA (bottom) antibodies. Lane 1, 10% input control.

(B) KSHV latently-infected BC2 PEL cells were treated with TPA (20 ng/ml) for 48 hr and MG132 (0.5 μM) for the final 16 hr, then whole-cell lysates were immunoprecipitated with control antibody IgG (lane 2), anti-IRF7 PAb (lane 3), or anti-RTA PAb (15% input) (lane 4) and immunoblotted with anti-RTA PAb. Lane 1, 5% input control.

(C) RTA binds to IRF7 in vitro. [^{35}S]-labeled MYC-RTA(1–544) and [^{35}S]-HA-IRF7(138–503) were each synthesized by in vitro transcription-translation and tested for binding by coimmunoprecipitation with either anti-HA, anti-MYC epitope, or control IgG antibodies as indicated. Lanes 1 and 2, single input protein controls without immunoprecipitation; lanes 3–5, mixture of both proteins incubated together before immunoprecipitation with either anti-MYC, anti-HA, or a nonspecific Ab (IgG); lanes 6 and 7, single protein negative controls showing MYC-RTA immunopreciptated with anti-HA MAb and HA-IRF7 immunoprecipitated with anti-MYC MAb.

(D) In vitro GST affinity binding assay. Bacterially expressed GST alone (lane 1), GST-RTA(1–691) (lane 2), or the truncation mutant GST-RTA(1–273) (lane 3) attached to beads were incubated together with in vitro-translated [^{35}S]-IRF7(1–503).

by the Ub-proteasome pathway and that interaction of the KSHV RTA protein with IRF7 results in a powerful inhibitory effect on IRF7 transcriptional activation of both endogenous IFNα/β mRNA synthesis and IFNα/β-LUC promoter activity. The mechanism involves binding to and targeting of IRF7 for degradation in a proteasome-dependent manner and is mediated by an unconventional intrinsic Ub E3 ligase activity encoded by the N terminus of RTA. These results imply that the Ub-proteasome pathway regulates normal IRF7 turnover and show that its destabilization is greatly enhanced by interaction with RTA, which presumably contributes to a disruption of the induced antiviral state during the KSHV lytic cycle.

Results

KSHV RTA Binds to IRF7 in Cotransfected Cells, in KSHV-Infected Cells, and In Vitro

During a search for human lymphocyte proteins that bind to a truncated form of the RTA(1–544) protein with the yeast two-hybrid system, we recovered and identified a positive clone encoding a fragment of the human IRF7 protein (residues 138–503). Interaction between the full-size, intact 69 kDa IRF7(1–503) and 110 kDa RTA(1–691) proteins within mammalian cells was demonstrated by coimmunoprecipitation with either anti-IRF7 or anti-RTA antibodies in cotransfected 293T cells with IRF7 in excess (Figure 1A, lane 2). Similarly, extracts of BC2 PEL cells after treatment with TPA and MG132 (to induce RTA expression and reduce proteasome degradation, respectively) gave a typical doublet of 90 plus 110 kDa RTA bands detectable after IRF7 immunoprecipitation (Figure 1B, lane 3), thus confirming that RTA does bind to the endogenous IRF7 protein in KSHV lytically infected cells.

Next, [^{35}S]-MYC-RTA(1–544) and [^{35}S]-HA-IRF7(138–503) were synthesized by in vitro translation then incubated together and immunoprecipitated. Both proved to be present in the immunoprecipitates obtained with either anti-MYC or anti-HA epitope antibodies (Figure 1C, lanes 3 and 4), but not in the specificity control samples (lanes 5–7). Finally, in a GST affinity binding experiment (Figure 1D), the 69 kDa in vitro translated [^{35}S]-labeled IRF7(1–503) protein was found to bind strongly to purified intact GST-RTA(1–691), but not to a truncated N-terminal GST-RTA(1–273) fragment. These results indicate that critical residues in RTA for IRF7 binding map between residues 273 and 544, which is distinct from the N-terminal DNA binding and dimerization domain (1–273) and from the C-terminal activation domain (544–691).

RTA Specifically Inhibits the Biological Function of IRF7 in Inducing IFN Gene Expression

To ask whether there are any functional consequences of RTA and IRF7 interactions on type-I IFN gene expression, we used a real-time RT-PCR quantitative IFN mRNA assay. The wild-type (wt) IRF7(1–503) expression plasmid was introduced into 293T cells (which are known to have very low basal levels of IRF7) to induce endogenous IFNα and IFNβ mRNA synthesis. Sendai virus was used as a potential coinducer in the experiments shown but proved to have little added effect on IRF7 function in these assays. Three primer pairs that detect just IFNα1 mRNA, a consensus for 12 IFNα gene

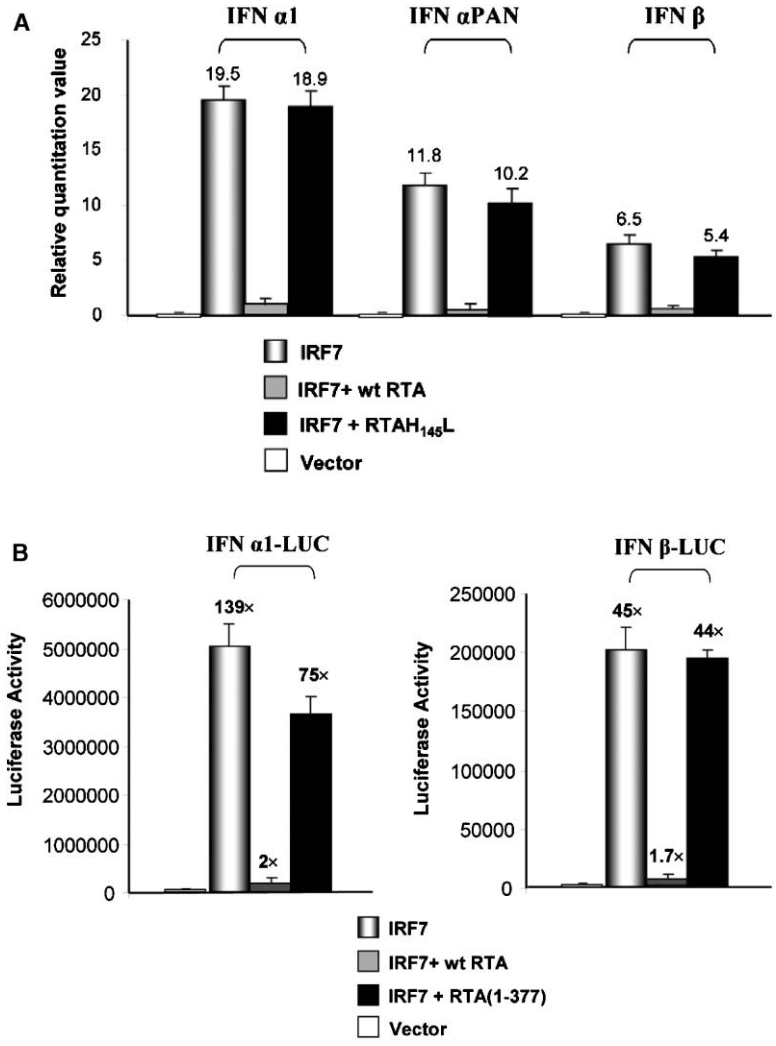

Figure 2. Inhibition of IRF7-Induced IFN mRNA and IFN-LUC Levels by Cotransfected RTA

(A) The histograms depict the levels of induction of IFNα1, Pan IFNα (consensus primers), and IFNβ mRNA produced 48 hr after transfection of 293T cells: (1) control vector DNA; (2) wt IRF7(1–503) expression plasmid DNA alone; or (3) and (4) IRF7 plus cotransfected wt RTA(1–691) or mutant RTA(H145L) plasmid DNA. All samples included Sendai virus infection for 16 hr. The relative quantitative values of the results from SYBR Green real-time RT-PCR assays are shown as fold increase of IFN mRNA levels over basal levels obtained with empty plasmid vector DNA in the absence of either IRF7 or RTA.

(B) Effect of RTA on IRF7-induced gene expression from reporter luciferase (LUC) genes driven by the IFNα and IFNβ promoters after transfection into 293T cells. Target IFNα1-LUC or IFNβ-LUC plasmids were cotransfected either with (1) vector alone; (2) IRF7 (1–503) alone; (3) IRF7 plus RTA(1–691), or (4) IRF7 plus RTA(1–377). At 24 hr after transfection, cells were infected with Sendai virus for 12 hr before harvesting for LUC assays. The measured LUC activity is shown as fold increases over the basal level obtained with just target DNA and empty vector control DNA in the absence of either the IRF7 or RTA expression plasmids.

mRNAs (pan IFNα), or IFNβ mRNA measured 19.5-, 11.8-, and 6.5-fold induction, respectively, by IRF7 over basal mRNA levels with vector plasmid and Sendai alone (Figure 2A). However, the effect of IRF7 was nearly completely abolished by cotransfection with a wt RTA(1–691) expression plasmid. Importantly, an RTA point mutant with His145 changed to Leu (see later) failed to have any significant inhibitory effect.

As an alterative measure of interference with IFN transcriptional activation, we also carried out luciferase (LUC) reporter gene assays. The basal levels of target IFNα1-LUC or IFNβ-LUC gene activity in 293T cells were boosted 139- and 45-fold by adding cotransfected IRF7(1–503) in the presence of Sendai virus (Figure 2B). However, inclusion of cotransfected RTA(1–691) nearly completely reversed the effect, with a measured inhibition of 70-fold and 26-fold, respectively. In this case, an RTA(1–377) truncation mutant that both lacks the C-terminal transactivator domain and fails to bind to IRF7 served as the negative control. This result contrasts dramatically with the strong positive transactivation effect of RTA on its direct viral target promoters in similar assays (Wang et al., 2003).

RTA Alters the Nuclear and Cytoplasmic Distribution of Cotransfected IRF7

IRF7 is considered to be an intrinsically cytoplasmic protein that needs modification and conformational activation to be translocated into the nucleus where it functions as a DNA binding transcription factor (Au et al., 1998; Lin et al., 2000). In contrast, RTA is a predominantly nuclear protein. To visualize the intracellular localization patterns of singly and cotransfected RTA and IRF7, we carried out double-label IFA in 293T cells in the absence and presence of Sendai virus to enhance the IRF7 nuclear activation. FLAG-tagged IRF7 alone proved to be significantly less abundant in the nucleus than in the cytoplasm (Figures 3A–3C), although Sendai virus infection increased the nuclear localization by several fold (Figures 3D–3F). In contrast, in the cultures that were cotransfected with IRF7 and RTA in the presence of Sendai virus infection, IRF7 staining was lost completely from the nucleus in all cells as well as from the cytoplasm in about half of those cells that were also positive for RTA (Figures 3G–3I), although the nuclear distribution of RTA was unaffected. The merge patterns of IRF7 and RTA expression in one typical coexpressing cell showing a complete

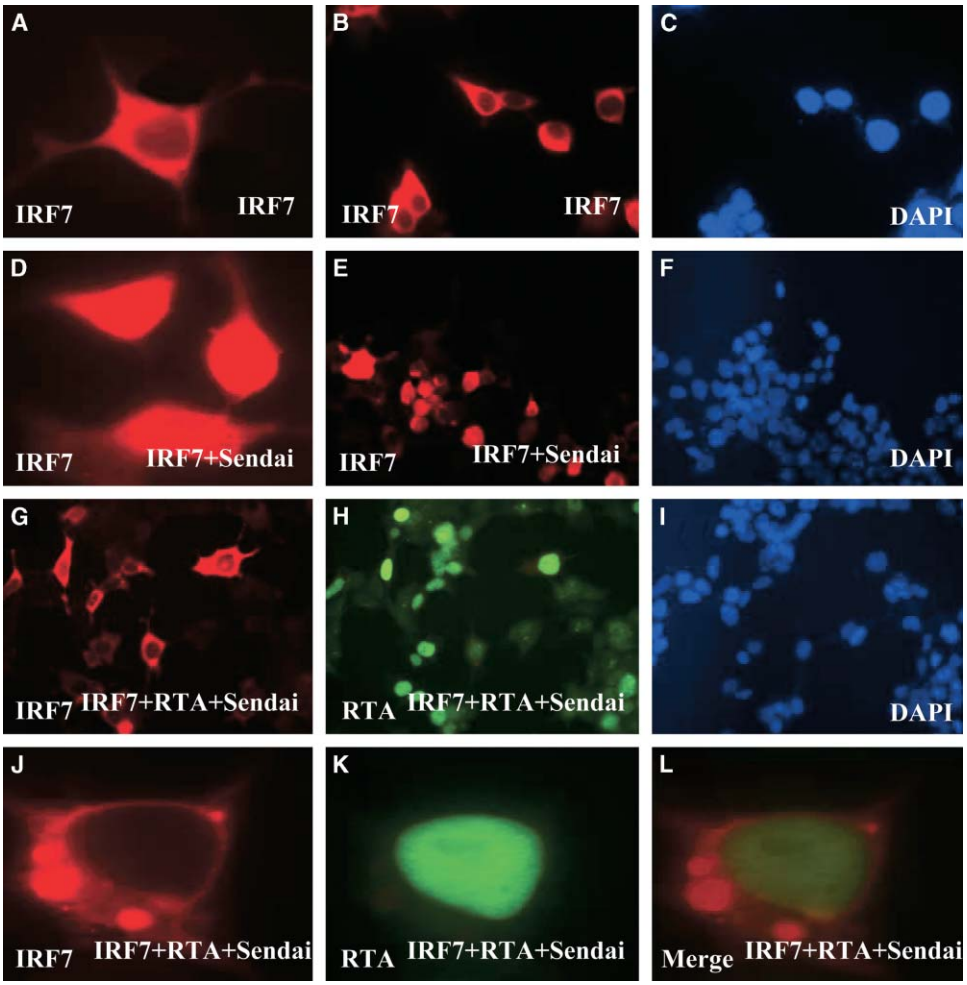

Figure 3. Cotransfected RTA Alters the Intracellular Localization of the IRF7 Protein

293T cells were transfected with FLAG-IRF7(1–503) alone (A–C), or infected with Sendai virus for 12 hr (D–F), or cotransfected with FLAG-IRF7 plus RTA(1–691) and infected with Sendai virus (G–I). A higher power image of one representative selected RTA-positive cell showing residual IRF7 in the cytoplasm but none in the nucleus is shown in (J)–(L). Single or double-label IFA with anti-FLAG MAb (red) or anti-RTA PAb (green) was performed revealing some increased translocation of IRF7 to the nucleus in the presence of Sendai virus but the frequent absence of IRF7 from the nucleus (and sometimes the cytoplasm as well) in cells that also expressed RTA. All cell nuclei in the fields are shown by DAPI staining (blue in [C], [F], and [I]) and a merge of frames (J) and (K) is shown in (L).

absence of IRF7 from the nucleus, but not from the cytoplasm, are also shown at high power (Figures 3J–3L). Given that RTA interacts physically with IRF7, we expected to observe an increased nuclear sequestration of IRF7 in the presence of RTA but, instead, there appeared to be preferential exclusion or degradation of presumably RTA-bound nuclear IRF7.

RTA Promotes IRF7 Degradation via the Ub-Proteasome Pathway

To examine whether ectopic expression of RTA could affect the levels of IRF7 protein produced, we cotransfected increasing amounts of the RTA plasmid together with a constant amount of the FLAG-IRF7 plasmid. Indeed, inclusion of RTA proved to decrease the level of recovered IRF7 protein detected by immunoblotting in an inverse, dose-dependent manner (Figure 4A, lanes 1–7). However, in the presence of the proteasome inhibitor MG132, the reduction of IRF7 protein levels was nearly completely reversed (lane 8), although MG132 had little effect in the absence of RTA (lane 10). Therefore, the ability of MG132 to restore the levels of IRF7 indicates that RTA may indeed promote the degradation of IRF7 via the Ub-proteasome pathway. Interestingly, the RTA protein levels themselves also decreased at the highest input plasmid levels used (lanes 6 and 7), and MG132 substantially increased the RTA protein levels (lane 8), suggesting that RTA may negatively autoregulate its own proteasome-mediated stability. Importantly, cotransfection with mutant RTA(H_{145}L) or truncated RTA(1–377) failed to inhibit the accumulation of untagged, intact IRF7(1–503) (Figure 4B, bottom). The RTA (H_{145}L) point mutant also proved to be more stable than wt RTA (top). Similar experiments to address the target specificity with either STAT1 or IRF1 revealed no effects of cotransfected RTA on their protein levels nor of MG132 on Flag-IRF7 levels obtained in the absence of RTA (Figure 4C).

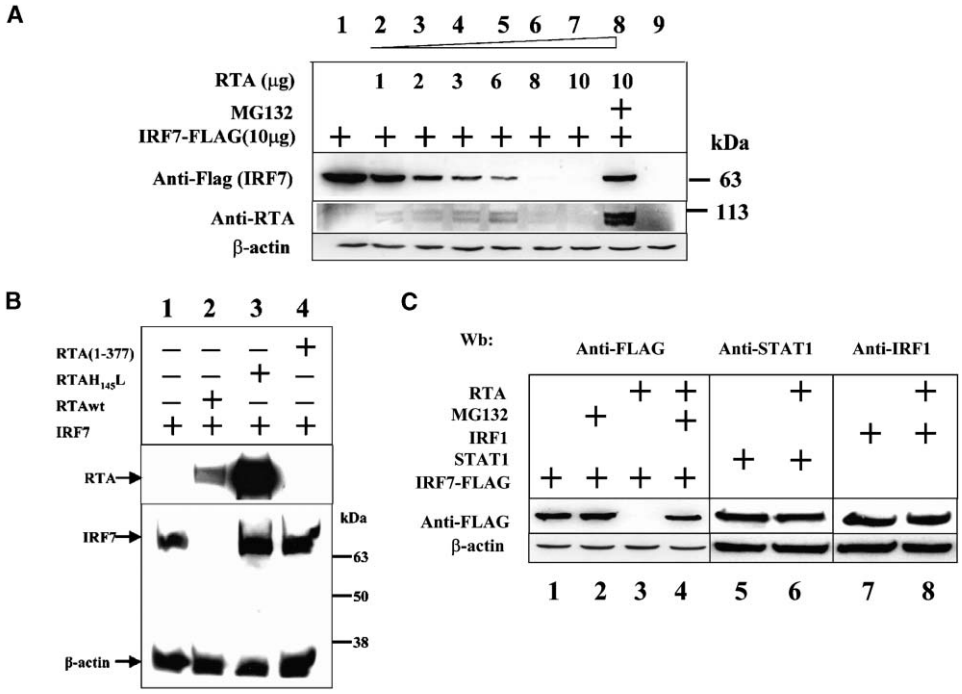

Figure 4. Cotransfected RTA Reduces the Levels of IRF7 Protein in a Proteasome-Dependent Manner

(A) Dose response assay for intracellular degradation of both IRF7 and RTA. Lanes 1–7, 293T cells were cotransfected with 10 ug of FLAG-IRF7 plus the indicated amounts of RTA plasmid DNA (1–10 ug) in the absence of Sendai virus, then WCE were prepared and immunoblotted with anti-FLAG (top), anti-RTA (center) or anti-β-actin (bottom) antibodies. Lane 8, same as lane 7 except treated with MG132 at 0.6 nM for 24 hr after transfection. Lane 9, untransfected cell extract control.

(B) Inactivation of RTA-mediated inhibition of IRF7 levels by mutagenesis. The indicated wt or mutant RTA expression plasmids were cotransfected into 293T cells together with wt untagged IRF7. Whole-cell lysates were then subjected to immunoblotting to detect the RTA protein (top) or to detect the IRF7 and β-actin proteins (bottom).

(C) Specificity of RTA mediated degradation: 293T cells were transfected with expression plasmids (10 μg each) encoding Flag-IRF7, IRF1, or STAT1 alone (lanes 1, 2, 5, and 7) and in the presence of cotransfected wt RTA (lanes, 3, 4, 6, and 8) or of added MG132 (lanes 2 and 4). WCE were immunoblotted with anti-FLAG, anti-IRF1, or anti-STAT1 MAb as indicated.

Role of Phosphorylation and of a Cys/His-Rich Domain of RTA

To evaluate whether RTA has preferential effects on phosphorylated IRF7, ectopic FLAG-IRF7 was expressed in 293T cells with or without cotransfected wt RTA in the presence or absence of Sendai virus and separated into both nuclear and cytoplasmic fractions. Immunoblotting with anti-FLAG antibody (Figure 5A) detected almost exclusively the slower mobility phosphorylated form of IRF7 (P-IRF7) in the nucleus in both the presence and absence of Sendai virus, whereas the cytoplasmic fraction contained two closely migrating bands of nearly equal abundance representing both phosphorylated and unphosphorylated forms of IRF7. Added RTA proved to greatly reduce the levels of both nuclear and cytoplasmic IRF7, although there was clearly some preferential degradation of phosphorylated over unphosphorylated IRF7 in the cytoplasmic fraction.

A deleted version of IRF7(Δ 477–479), which lacks two key Ser residues and is both unable to respond to Sendai virus induced nuclear translocation and is functionally impaired in IFNα1-LUC reporter assays (Lin et al., 2000), was nevertheless still completely degraded just as effectively as the wt form by cotransfected RTA in the absence of Sendai virus (Figure 5B). Therefore, although the phosphorylated forms of IRF7 appear to be somewhat preferentially degraded by RTA, modification at Ser 477 or 479 is clearly not required.

The region of RTA from positions 118–207 encompass a cluster of six Cys and one His residues. To ask whether this domain might play a role in the degradation of IRF7, we used site-directed mutagenesis to generate three point mutants in which either Cys or His were converted to Ser or Leu by single nucleotide changes. In contransfection experiments in 239T cells, mutants $C_{131}S$, $C_{141}S$, and $H_{145}L$ as well as RTA(1-377) all proved to be inactive in decreasing both nuclear and cytoplasmic FLAG-IRF7 protein levels (Figure 5C, top). Two of these point mutants also gave more abundant (and presumably more stable) RTA protein levels than did wt RTA(1–169), especially in the cytoplasm (Figure 5C, bottom).

Detection of Polyubiquitin-Conjugated Forms of Endogenous IRF7 and Stabilization by a Proteasome Inhibitor

To evaluate the hypothesis that turnover of IRF7 may normally be regulated by the Ub-proteasome pathway, endogenous IRF7 levels were determined in both HeLa cells and the human B cell line DG75 before and after treatment with MG132 (Figure 6A). As expected, only a small amount of IRF7 was detected in the absence of the proteasome inhibitor; however, steady-state levels

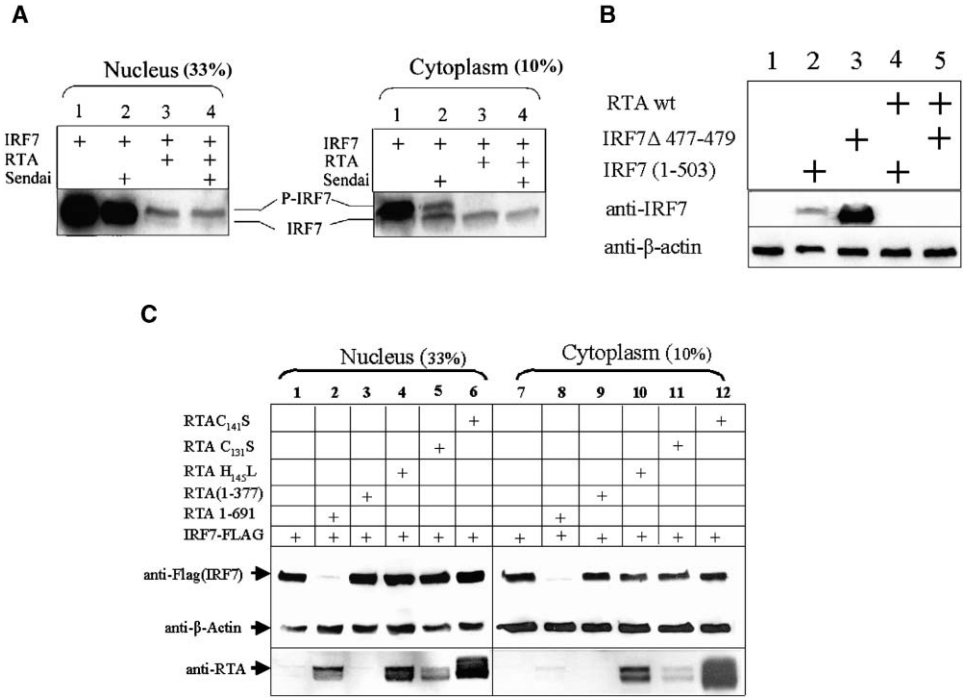

Figure 5. Degradation of IRF7 Requires an N-Terminal His/Cys-Rich Domain of RTA and Occurs in Both the Nucleus and Cytoplasm and with or without Phosphorylation

(A) Nuclear versus cytoplasmic and phosphorylated forms. 293T cells were transfected with the indicated plasmids (10 μg each). Sendai virus was added at 16 hr to one-half of the culture, and the cells were harvested at 30 hr and immunoblotted for IRF7. The nuclear and cytoplasmic fractions shown represent 33% and 10% of the lysates, respectively. The upper phosphorylated (P-IRF) and lower unphosphorylated forms of IRF7 are indicated.

(B) A nonphosphorylatable form of IRF7 is still susceptible to RTA degradation. To compare the effects of RTA on wt IRF7(1–503) and phosphorylation-deficient mutant IRF7(Δ477/479), 293T cells were transfected with the indicated target plasmids either with or without cotransfected RTA(1–169) and WCE were immunoblotted with either anti-IRF7 PAb (top) or with anti-β-actin MAb (bottom).

(C) Requirement for the Cys plus His-rich N-terminal region of RTA. 293T cells were cotransfected with FLAG-IRF7 together with either empty plasmid only, wt RTA, the three RTA point mutants, or the RTA(1–377) truncation mutant. Cell extracts were separated into nuclear (33%) and cytoplasmic (10%) fractions and immunoblotted with either anti-FLAG (top), anti-β-actin (center), or anti-RTA (bottom).

of IRF7 were significantly increased in cells exposed to even the lowest level of MG132 tested. To directly measure the stability of transfected wt IRF7(1–503) in 293T cells, we next carried out immunoblotting of standard whole-cell extracts (WCE) after addition of cycloheximide (CHX) to block all new protein synthesis (Figure 6B). In the absence of MG132 (top), the levels of IRF7 decreased linearly with a measured half-life of 2 hr, whereas in the presence of MG132 (bottom), the IRF7 protein stability was increased 4- to 5-fold. This result confirms that IRF7 is a moderately unstable protein in transfected 293T cells and clearly implies that it is subject to proteasome-mediated negative regulation.

To examine directly whether endogenous IRF7 is indeed subject to polyUb conjugation, DG75 cell extracts were prepared by gentle sonication in RIPA buffer as appropriate for endogenous in vivo ubiquitination assays. Strikingly, high molecular weight protein smears were detected after IRF7 immunoprecipitation by both the anti-Ub and anti-IRF7 antibodies (Figure 6C). Importantly, treatment with MG132 for 16 hr at 0.5 μM (lane 3), but not mock treatment (lane 2), enhanced the accumulation of Ub-IRF7 conjugates. Very similar results were obtained for immunoprecipitated endogenous Ub-IRF7 forms in HeLa cells, as well as by immunoprecipitation of FLAG-IRF7 after cotransfection with HA-tagged Ub into 293T cells in the presence of MG132 (data not shown).

Finally, when IRF7(1–503), IRF7(1–151), and IRF7(152–503) were each cotransfected with pHA-Ub into 293T cells, and the levels of in vivo ubiquitination were compared after sonication in RIPA buffer, only immunoprecipitated wt IRF7(1–503) proved to be heavily conjugated to polyUb, although IRF7(1–151) retained some polyUb adducts (Figure 6D). Therefore, both N-terminal and C-terminal segments of IRF7 are evidently required for polyUb-conjugation.

RTA Promotes the Proteasome-Mediated Degradation of PolyUb-Conjugated IRF7 in Cotransfected Cells

To test whether RTA directly promotes the degradation of IRF7 by enhancing the Ub-mediated pathway, exogenous FLAG-IRF7(1–503) together with RTA(1–691) or RTA(H_{145}L) were cotransfected together with pHA-Ub into 293T cells for an intracellular ubiquitination assay. In the absence of RTA, a slowly migrating high molecular weight smear of polyUb-IRF7 was observed (Figure 7A,

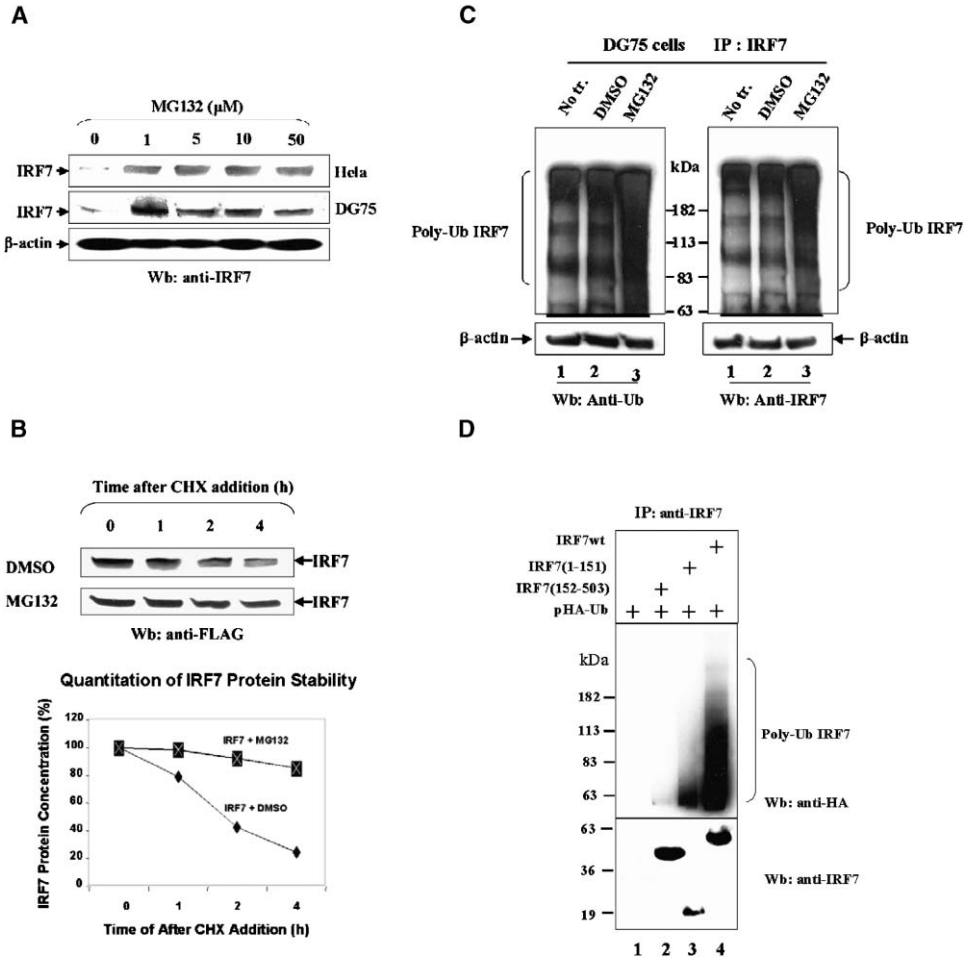

Figure 6. Stabilization of Endogenous IRF7 Protein with the Proteasome Inhibitor MG132 and Detection of PolyUb-Conjugated IRF7 In Vivo

(A) Stabilization, HeLa and DG75 cells were exposed to TPA at 20 ng/ml to stimulate the expression of IRF7 for 24 hr and then either treated or mock treated with MG132 at different concentrations as indicated for 6 hr. Standard whole-cell lysates were immunoblotted with anti-IRF7 PAb.

(B) Measurement of the half-life of transfected IRF7 protein. The expression plasmid encoding wt IRF7(1–503) was transfected into 293T cells, and cycloheximide (CHX) was added at 40 hr to block all new protein synthesis. Standard WCE were prepared at 0, 1, 2, and 4 hr either in the presence of 0.5 μM MG132/0.1% DMSO or in the presence of 0.1% DMSO solution alone as control and immunoblotted with anti-IRF7 PAb (top). The band intensities on the exposed film are plotted graphically on the bottom.

(C) Endogenous IRF7 is conjugated to polyUb in vivo. DG75 cells were either untreated (No tr, lane 1), mock treated (DMSO, lane 2), or exposed to 0.5 μM MG132/0.1% DMSO for 16 hr. WCE were prepared by sonication in RIPA buffer for in vivo ubiquitination assays, then immunoprecipitated with anti-IRF7 antibody followed by immunoblotting with either anti-Ub MAb (top left) or with anti-IRF7 PAb (top right), and later reprobed with anti-β-actin MAb (bottom).

(D) Mapping of the target region of IRF7 for endogenous polyUb-conjugation. In vivo ubiquitination assays were carried out with WCE prepared from 293T cells by sonication in RIPA buffer after cotransfection with pHA-Ub and a control plasmid (lane 1) or each of the three indicated wt or deleted IRF7 expression plasmids (lanes 2–4). IRF7 was immunoprecipitated from the extracts with anti-IRF7 PAb and then immunoblotted with either anti-HA MAb (top) or with anti-IRF7 PAb (bottom).

lanes 3 and 4). However, a strikingly reduced level of both IRF7 conjugates and unmodified IRF7 was obtained when wt RTA(1–691) was cotransfected in the absence of MG132 (lane 5), implying that greatly enhanced proteasome-mediated degradation of polyUb-IRF7 had occurred. Treatment with MG132 led to substantial rescue of both the high molecular weight IRF7 conjugates and unmodified IRF7 in the presence of RTA (lane 6), but coexpression of FLAG-IRF7 with mutant RTA(H_{145}L) had no effect (lanes 7 and 8). These findings provide clear evidence that RTA promotes IRF7 degradation via proteasome-mediated degradation of polyUb-conjugated forms of IRF7 in cotransfected cells.

RTA Functions as a Ub E3 Ligase for IRF7 In Vitro in Concert with the UbcH5α E2 Enzyme

To confirm that RTA itself functions directly to add polyUb to IRF7, the E3 Ub ligase activity of RTA was assessed by performing in vitro cell-free ubiquitination assays with purified bacterial GST-IRF7 (3 μg) as substrate and GST-RTA added in catalytic amounts (80 ng). Incubation together with the other standard compo-

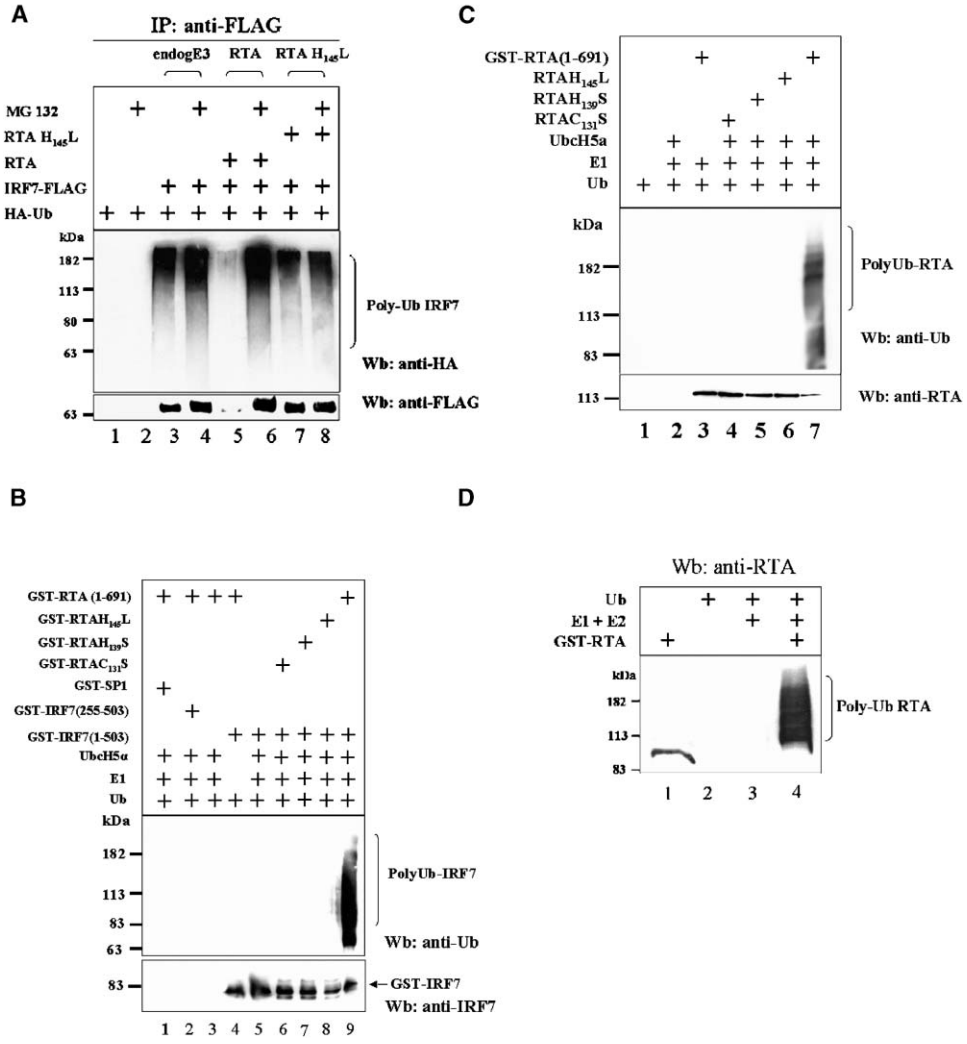

Figure 7. RTA Promotes the Ubiquitination of Both IRF7 and Itself In Vitro and the Degradation of PolyUb-IRF7 In Vivo

(A) Intracellular ubiquitination assay. 293T cells were transfected with pHA-Ub and FLAG-tagged IRF7 together with the indicated RTA expression plasmids. Whole-cell lysates prepared by sonication in RIPA buffer were immunoprecipitated with anti-FLAG PAb and immunoblotted first with anti-HA MAb to detect polyUb-conjugated forms of IRF7 (top) and then reprobed with anti-FLAG MAb to detect unmodified IRF7 (bottom).

(B) In vitro polyUb-conjugation of IRF7 by RTA. Cell free in vitro ubiquitination reactions were carried out by incubation of the indicated purified protein components. Input GST-RTA samples were used at catalytic levels (80 ng), whereas GST-IRF7 was used at substrate levels (3 ug). Immunoblotting was performed to detect polyUb-conjugated and unconjugated 90 kDa GST-IRF7 by using either anti-Ub MAb (top) or anti-IRF7 PAb (bottom).

(C) RTA exhibits self-polyUb conjugation activity. Cell free in vitro ubiquitination assays were carried out by incubation of the indicated purified protein components. Input GST-RTA samples were used at substrate levels (3 ug). Western blotting was used to detect polyUb-conjugated RTA with anti-Ub MAb (top) or with anti-RTA PAb (bottom).

(D) Direct detection of polyUb-conjugated RTA in vitro. Cell free in vitro ubiquitination assays with substrate level input amounts of wt GST-RTA were carried out as in (C), except that the high molecular forms of RTA (lane 4) were detected with anti-RTA PAb on the same blot as the unmodified form (lane 1).

nents including Ubc5Hα (Figure 7B) produced high molecular weight Ub-containing products conjugated to the GST-IRF7 protein as detected with anti-Ub mouse monoclonal antibodies (MAb) (top) but did so only in the sample containing the complete reaction components (lane 9). Confirmation of the presence of the intact 90 kDa GST-IRF7(1–503) protein by Western blotting with anti-IRF7 antibody is shown on the bottom. Omission of GST-RTA (lane 5), GST-IRF7 (lane 3), or E1 plus Ubc5Hα (lane 4) all failed to yield any polyUb-conjugated bands. Furthermore, all three Cys/His point mutants of GST-RTA were inactive, and substitution with either purified GST-SP1 protein or the deleted GST-IRF7(255–503) protein, instead of GST-IRF7(1–503) as targets, also failed to produce any polyUb-containing products. This result provides unambiguous evidence that the N terminus of

RTA contains an intrinsic E3 Ub ligase catalytic domain that functions together with the UbcH5A E2 enzyme to specifically ubiquitinate IRF7.

RTA Also Catalyses Self-Ubiquitination In Vitro

To assess whether RTA may be capable of autoregulation, a similar cell-free in vitro assay was carried out with purified components, but this time by using substrate level amounts of GST-RTA (3 μg) without any added IRF7 protein (Figure 7C). Again, E2-dependent Ub ligase activity was detected only in the reaction containing all four bacterial-derived components, namely Ub, E1, UbcH5α, and wt GST-RTA(1–169), but not in the absence of either GST-RTA or UbcH5A. Substitution with any of the three GST-RTA Cys/His region point mutants failed to produce a high molecular weight GST-RTA smear. Further confirmation that the high molecular weight HA-polyUb containing bands observed in vitro do indeed represent polyUb-conjugated forms of RTA itself was obtained by immunoblotting with anti-RTA antibody (Figure 7D). The resulting high molecular weight forms of RTA were only generated after incubation in the presence of E1, E2, and Ub, but not in their absence nor in the absence of GST-RTA. These results affirm that RTA is indeed able to catalyze self-ubiquitination in vitro and that this self-catalyzed activity requires the same Cys plus His-rich region involved in polyUb conjugation to IRF7.

Discussion

Normal Control of IRF7 Protein Levels via the Ub-Proteasome Pathway

Our evidence here clearly indicates that the levels of accumulation of the relatively short half-lived IRF7 protein are tightly regulated by the Ub-proteasome pathway in normal human cells, presumably under the control of a specific cellular Ub E3 ligase. Although polyUb-conjugation of IRF1 (Nakagawa and Yokosawa, 2000) and sensitivity of IRF3 to proteasome inhibitors (Lin et al., 1998) have been described, the mechanism for controlling the endogenous activity and turnover of IRF7 has not previously been addressed. Evidently, KSHV exploits this pathway to block IRF7 function and the KSHV RTA transcription factor has also evolved an enzymatic domain that has functional parallels with the predicted cellular Ub E3 ligase for IRF7.

Mechanism of RTA-Mediated Regulation of IRF7 Protein Stability

Although phosphorylation may contribute to enhancement of the RTA-mediated Ub-dependent degradation of IRF7 in vivo, the preference is clearly not an absolute requirement because firstly, at the highest ratios of RTA to IRF7 used in many of our cotransfection experiments, all IRF7 protein present in the both the nucleus and cytoplasm was degraded (e.g., see Figures 4B, 5B, and 5C). Secondly, deletion of the two key phosphorylated Ser residues at position 477 and 479 in IRF7 did not prevent RTA-mediated degradation (Figure 5C) Thirdly, efficient IRF7 ubiquitination of presumably unphosphorylated GST-IRF7 was observed in vitro (Figure 7B). To understand how apparently cytoplasmic forms of IRF7 are degraded in the presence of nuclear RTA in cotransfected cells, we will probably need to determine whether binding of IRF7 to RTA is itself sufficient to translocate IRF7 into the nucleus. In contrast, the predicted cellular E3 Ub ligase for IRF7 seems likely to function in the cytoplasm in the absence of Sendai virus-induced effects.

It has been reported that removal of an apparent inhibitory region at the C terminus of IRF7 in IRF7(Δ247–467) gives 40-fold stimulation of IFNα-LUC transactivation in the absence of Sendai virus (Lin et al., 2000). Therefore, this might correspond to part of the region that is targeted for destabilization by the cellular UbE3L. As might be expected, we initially had considerable difficulty in demonstrating an interaction between RTA and IRF7 in both BC2 PEL cells and in cotransfection experiments, but the realization that targeting of IRF7 by RTA led to its degradation allowed us to adjust the conditions by using the proteasome inhibitor in BC2 cells and high input ratios of IRF7 to RTA in the cotransfection experiments.

Role of the Cys Plus His-Rich Region of RTA in the Degradation of IRF7 and Self-Ubiquitination

Our results indicate that KSHV RTA specifically targets the IRF7 protein for proteasome degradation, whether in the nucleus or cytoplasm, thus greatly reducing the steady-state levels of activated IRF7 protein and abolishing transcriptional stimulation of IFNα and IFNβ mRNAs. The ability of RTA to target both IRF7 and itself for polyUb conjugation and subsequent proteasome-mediated degradation strongly implies that RTA, like the cellular HPV E6-associated E6-AP (Scheffner et al., 1993), the HSV-encoded ICP0 (Boutell et al., 2002; Hagglund et al., 2002), and the KSHV-encoded MIR1 (K3) and MIR2 (K5) proteins (Coscoy and Ganem, 2003), possesses an intrinsic E3 ligase activity. Autoubiquitination is a common feature of some E3 ligases and is therefore a good indicator of intrinsic E3 activity. Three key residues, Cys_{131}, Cys_{141}, and His_{145}, were identified that are each absolutely required for promoting the degradation of IRF7 as well as for RTA self-ubiquitination. Importantly, all three of the RTA catalytic region point mutants still retain their ability to bind to both the IRF7 and C/EBPα proteins and to bind to target RRE DNA motifs in EMSA experiments (data not shown). They also retain about 70% of their normal level of transactivation of viral target promoters, suggesting that these mutants specifically abrogate only the E3 ligase function of RTA. Although the proposed intrinsic RTA E3 ligase catalytic activity encompasses a novel Cys-rich region from amino acids 118–207 (Cys3HisCys3), sequence comparisons show no significant similarity between this domain and any previously described conserved E3 ligase domains.

There are two distinct types of E3 ligase known: the enzymatic HECT domain E3s and the zinc finger domain E3s, including two classes of RING-finger related domains, the U box and PHD domain E3s. The recognition that RING finger proteins can bind E2 enzymes in a specific and catalytically productive manner represented

a major advance in Ub biochemistry (Pickart, 2000). A number of RING or PHD domain containing viral Ub E3 ligases have been identified, including HSV-encoded ICP0 (the prototype classic RING-finger protein) and a subclass of KSHV-encoded membrane-bound PHD proteins (vMIR1 and vMIR2) that target MHC class I degradation (Coscoy and Ganem, 2003; Ishido et al., 2000). Unlike the HSV ICP0 immediate-early nuclear protein, which has E3 ligase activity but for which only substrate-independent formation of polyUb has been demonstrated so far in vitro (Boutell et al., 2002; Hagglund et al., 2002), we have obtained clear evidence here for specific Ub-conjugation of the target IRF7 protein in vitro by the RTA Ub E3 ligase activity.

A variant, noncanonical Cys plus His rich domain associated with E3 activity was described recently in the Mumps virus V protein that degrades STAT1 in a ubiquitin-dependent manner (Yokosawa et al., 2002). Therefore, functional E3 protein domains may not be limited just to the currently known motifs, and KSHV RTA may represent another variant of Cys plus His-rich E3 ligases.

Targeting Specificity of RTA Ub E3 Ligase Activity

A central domain of RTA between amino acids 273–544 binds to IRF7 and presumably brings it into proximity with the adjacent RTA catalytic region. When most of this segment was deleted in RTA(1–377), both the targeted ubiquitination and degradation of IRF7 were abolished, despite the continued presence of the N-terminal catalytic domain. This organization resembles that in E6-AP which is well known to target p53 for degradation by the Ub-proteasome pathway in association with HPV E6 (Scheffner et al., 1993).

To begin to evaluate whether RTA may have a broader target specificity than just IRF7, we have also carried out preliminary experiments to test whether cotransfection with RTA negatively affects the accumulation of other IRFs and transcription factors. The results showed that cotransfection with RTA also leads to degradation of IRF3 (data not shown) but has no effect on IRF1 or STAT1 protein levels. In contrast, as described previously, the C/EBPα level was significantly elevated by coexpressed RTA (Wang et al., 2003).

The discovery that RTA itself has an unconventional intrinsic Ub E3 ligase activity is even more remarkable considering that one of the other RTA binding cellular proteins recovered from the yeast two-hybrid library screen was a HECT domain Ub E3 ligase protein. We have found that this cellular protein not only binds to both RTA and IRF7 but also catalyses polyUb-conjugation and proteasome-dependent degradation of IRF7 and IRF3 (Y.Y. and G.S.H., unpublished data). This may well be the predicted cellular Ub E3 ligase for IRF7. Therefore, RTA may both act as an E3 ligase itself to specifically target IRF7 for destruction via the Ub-proteasome pathway, as well as recruit and modulate a cellular E3 ligase that regulates IRF-related pathways.

Possible Role in KSHV-Infected Cells

All of our data here argue that RTA by itself can specifically and very efficiently target IRF7 for degradation both in the nucleus and less efficiently in the cytoplasm, which could account for the absence of IFN mRNA induction in KSHV-infected endothelial cell cultures despite the strong induction of the mRNAs for IRF7 and many other ISGs (Poole et al., 2002). Nevertheless, KSHV infection itself probably has additional redundant levels of response to cellular antiviral effects. For example, two other KSHV-encoded early lytic cycle proteins have been implicated as negative regulators of IRF responses. vIRF1 inhibits IRF1 by competing for binding to p300 (Gao et al., 1997; Li et al., 2000; Zimring et al., 1998), and ORF45 specifically binds to IRF7 and may sequester it in the cytoplasm (Zhu et al., 2002). Our functional transfection assays for inhibition of IFN mRNA synthesis by RTA gave at least 10-fold stronger effects than were reported by any of these other studies, but whether RTA-mediated processes are truly more dominant in KSHV-infected endothelial and B lymphocyte cells remains a subject for future evaluation.

Experimental Procedures

Plasmids and Expression Vectors

Expression plasmids encoding IRF7A(1–503), FLAG-IRF7A(1–503), GST-IRF7(1–503), and GST-IRF7(255–503) and reporter plasmids encoding firefly luciferase (LUC) under the control of human *IFNα1* ($-140/+9$) and *IFNβ* ($-280/+20$) promoter elements were provided by Yan Yuan (Zhu et al., 2002). Similar CMV-enhancer driven expression plasmids (pYXY7 and pYXY8) encoding IRF7(1–151) or IRF7(152–503) were generated by deletion from the parent intact IRF7(1–503) version. Mammalian expression plasmids pJX15 and pSEW-R01 encode full length cDNA versions of RTA(1–691) driven by the SV40 or HCMV enhancer-promoter regions. The RTA(1–377) C-terminal truncation mutant in plasmid pSEW-R03, GST fusion versions of full-length GST-RTA(1–691), GST-RTA(1–544), GST-RTA(1–377), and GST-RTA(1–273) were all described elsewhere (Wang et al., 2003). The GAL4-RTA(1–544) DNA binding domain fusion protein in plasmid pYXY1 was generated in the yeast vector pAS2-1 (Clontech) by PCR amplification from KSHV RTA cDNA.

Site-Directed Mutagenesis

Several point mutants in RTA(1–691) plasmid pSEW-R01 were created with the Quik-Change site-directed mutagenesis kit (Stratagene). The oligonucleotide primers used were as follows: $C_{131}S$ sense, 5′-GCATTTCTGACAGCCGCAAGCAGCGGGGTGAGCCTG CCT-3′; $C_{131}S$ antisense, 5′-AGGCAGGCTCACCCCGCTGCTTGCG GCTGTCAGAAATGC-3′; $C_{141}S$ sense, 5′-AGCCTGCCTCCAGCCAT ATCTAAGCTACTACACGAAATA-3′; $C_{141}S$ antisense, 5′-TATTTCGT GTAGTAGCTTAGATATGGCTGGAGGCAGGCT-3′; $H_{145}L$ sense, 5′-GCCATATGTAAGCTACTACTCGAAATATACACTGAGATG-3′; $H_{145}L$ antisense, 5′-CATTTCGGTGATTATTTCGAGTAGTAGCTTACATAT GGC-3′. These were used to create plasmids pYXY4, pYXY5, and pYXY6 encoding RTA(1–691/$C_{131}S$), RTA(1–691/$C_{141}S$), and RTA(1–691/$H_{145}L$), respectively. The same mutations were also all moved into the GST-RTA(1–691) background to create plasmids (pYXY 9, 10, and 11).

Antibodies

MAb against β-actin, FLAG (M2), HA, and MYC-epitopes were purchased from Sigma. Rabbit polyclonal antibody (PAb) against GST-IRF7(1-390), FLAG-epitope, and ubiquitin were purchased from SantaCruz (SC9053) or Sigma. Rabbit anti-peptide PAb recognizing RTA residues 527–539 was described previously (Wang et al., 2003).

Yeast Two-Hybrid Screening

The KSHV RTA bait plasmid (pYXY1) was cotransfected into AH109 yeast cells with a human EBV-infected lymphocyte cDNA library (Clontech, Matchmaker). Yeast colonies containing interacting proteins were identified by growth on media lacking Ade, His, Leu, and Trp and confirmed by assaying for β-galactosidase activity.

Cell Cultures, Transient Transfection, Indirect IFA, Nuclear, and Cytoplasmic Extracts and Immunoblotting

293T cells and HeLa cells were cultured in DMEM. The BC2 lymphoblastoid PEL cell line and the DG75 lymphoblast cell line (EBV and KSHV negative) were all maintained in RPMI medium. The KSHV lytic cycle in BC2 cells was induced by treatment with TPA (20 ng/ml) for 40 hr. Transient cotransfection assays by lipofection, IFA, separation of nuclear, and cytoplasmic fractions by NP40 lysis, and immunoblotting procedures were all performed as described elsewhere (Wang et al., 2003; Wu et al., 2003). In all experiments depicting nuclear versus cytoplasmic fractionation, the relative ratios of input sample used were 3.3 to 1.

In Vitro Coimmunoprecipitation

In vitro coimmunoprecipitation with [^{35}S]-labeled proteins was carried out by using the manufacturer's protocols (Clontech).

Intracellular Coimmunoprecipitation Assay, GST Affinity Binding Assay, LUC Reporter Assay, and In Vitro Transcription-Translation

These procedures were all described previously (Wang et al., 2003; Wu et al., 2003), except that MG132 (0.5 μM for 24 hr) was added to the BC2 cells to permit detection of IRF7 by coimmunoprecipitation with RTA.

Quantitative SYBR Green Real-Time RT-PCR

Details were described previously (Poole et al., 2002). PCR primers for IFNα1 and IFNβ were designed with GCG software (Genetics Computer Group). IFNα1 sense, 5′-AGAGCCCAAGGTTCAGAGTCA CCCATCTCAG-3′; IFNα1 antisense, 5′-AGCACCACCAGGACCATC AGTAAAGCAAAG-3′; IFNβ1 sense, 5′-CTCCAAATTGCTCTCCTGTT GTGCTTCTC-3′; IFNβ1 antisense, 5′-GCAGTATTCAAGCCTCCCA TTCAATTGCC-3′, IFNα Pan primers (consensus primer for all IFNα subtypes) (Zhu et al., 2002). Measurements were normalized relative to levels of 18S ribosomal RNA.

Cell-Free In Vitro Ubiquitination Assays

The standard reaction mixture (20 μl) contained 5 × PBDM buffer (50 mM Tris-HCL, [pH 7.6], 5 mM MgCl2, 2 mM ATP [including the regenerating system], and 0.3 U/ml inorganic pyrophosphatase), 40 ng of purified E1 protein (Boston Biochem), plus 200 ng of UbcH5α protein (Boston Biochem), 3 μg of bovine Ubiquitin (Sigma), 33 nM MG132 (Calbiochem), 5 μM Ub aldehyde (Boston Biochem), and appropriate amounts of purified GST-fusion proteins. As substrates, both GST-IRF7 (Figure 7B) and GST-RTA (Figure 7C) were used at 3 μg each (8 μl of undiluted extract), but as the E3 catalyst in Figure 7B, GST-RTA samples were used at 80 ng (2 ul of a 10-fold dilution of the same extract). Reaction mixtures were incubated for 2.5 hr at 37°C with agitation then separated on 8% SDS-PAGE gel and detected by ECL.

Intracellular IRF7 Degradation and Ubiquitination Assays

Either HeLa or DG75 cells were used directly for endogenous IRF7 studies or 293T cells were transfected with expression plasmids with or without proteasome inhibitor MG132 treatment (Calbiochem). For degradation assays, the cells were lysed at 24 hr after transfection with standard NP40 isotonic lysis buffer or with nuclear extract buffer, and equal amounts of protein were separated by 8% SDS-PAGE. Equal sample loading was verified by probing the membranes with anti β-actin MAb. For ubiquitination assays, the cells were transfected with pHA-Ub and indicated plasmids. After transfection, cells were treated with or without MG132 (0.5 μM) for 16 hr and then harvested by using RIPA buffer and sonication. Lysates were immunoprecipitated and subjected to 8% SDS-PAGE followed by immunoblotting.

Acknowledgments

These studies were funded by National Cancer Institute research grants (R01 CA73585 and P01 CA81400) to G.S.H. from the National Institutes of Health. We thank Yan Yuan (University of Pennsylvania, Philadelphia) for gifts of IRF7 expression plasmids and reporter genes; Ken Watanabe (National Institute for Longevity Science, Japan) for the pHA-Ub plasmid; and John Hiscott (McGill University, Montreal, Canada) for IRF7(Δ497/499). We also thank Cecile M. Pickart and Min Wang (Bloomberg School of Hygiene, Johns Hopkins University) for critically reading the manuscript and for technical advice.

Received: December 2, 2003
Revised: October 14, 2004
Accepted: November 17, 2004
Published: January 25, 2005

References

Au, W.C., Moore, P.A., LaFleur, D.W., Tombal, B., and Pitha, P.M. (1998). Characterization of the interferon regulatory factor-7 and its potential role in the transcription activation of interferon A genes. J. Biol. Chem. *273*, 29210–29217.

Boutell, C., Sadis, S., and Everett, R.D. (2002). Herpes simplex virus type 1 immediate-early protein ICP0 and is isolated RING finger domain act as ubiquitin E3 ligases in vitro. J. Virol. *76*, 841–850.

Chang, Y., Cesarman, E., Pessin, M.S., Lee, F., Culpepper, J., Knowles, D.M., and Moore, P.S. (1994). Identification of herpesvirus-like DNA sequences in AIDS-associated Kaposi's sarcoma. Science *266*, 1865–1869.

Coscoy, L., and Ganem, D. (2003). PHD domains and E3 ubiquitin ligases: viruses make the connection. Trends Cell Biol. *13*, 7–12.

Foy, E., Li, K., Wang, C., Sumpter, R., Jr., Ikeda, M., Lemon, S.M., and Gale, M., Jr. (2003). Regulation of interferon regulatory factor-3 by the hepatitis C virus serine protease. Science *300*, 1145–1148.

Gao, S.-J., Boshoff, C., Jayachandra, S., Weiss, R.A., Chang, Y., and Moore, P.S. (1997). KSHV ORF K9 (vIRF) is an oncogene which inhibits the interferon signaling pathway. Oncogene *15*, 1979–1985.

Goodbourn, S., Didcock, L., and Randall, R.E. (2000). Interferons: cell signalling, immune modulation, antiviral response and virus countermeasures. J. Gen. Virol. *81*, 2341–2364.

Hagglund, R., Van Sant, C., Lopez, P., and Roizman, B. (2002). Herpes simplex virus 1-infected cell protein 0 contains two E3 ubiquitin ligase sites specific for different E2 ubiquitin-conjugating enzymes. Proc. Natl. Acad. Sci. USA *99*, 631–636.

Hershko, A., and Ciechanover, A. (1998). The ubiquitin system. Annu. Rev. Biochem. *67*, 425–479.

Ishido, S., Wang, C., Lee, B.S., Cohen, G.B., and Jung, J.U. (2000). Downregulation of major histocompatibility complex class I molecules by Kaposi's sarcoma-associated herpesvirus K3 and K5 proteins. J. Virol. *74*, 5300–5309.

Kubbutat, M.H., Jones, S.N., and Vousden, K.H. (1997). Regulation of p53 stability by Mdm2. Nature *387*, 299–303.

Li, M., Damania, B., Alvarez, X., Ogryzko, V., Ozato, K., and Jung, J.U. (2000). Inhibition of p300 histone acetyltransferase by viral interferon regulatory factor. Mol. Cell. Biol. *20*, 8254–8263.

Liang, Y., Chang, J., Lynch, S.J., Lukac, D.M., and Ganem, D. (2002). The lytic switch protein of KSHV activates gene expression via functional interaction with RBP-Jkappa (CSL), the target of the Notch signaling pathway. Genes Dev. *16*, 1977–1989.

Lin, R., Heylbroeck, C., Pitha, P.M., and Hiscott, J. (1998). Virus-dependent phosphorylation of the IRF-3 transcription factor regulates nuclear translocation, transactivation potential, and proteasome-mediated degradation. Mol. Cell. Biol. *18*, 2986–2996.

Lin, R., Mamane, Y., and Hiscott, J. (2000). Multiple regulatory domains control IRF-7 activity in response to virus infection. J. Biol. Chem. *275*, 34320–34327.

Mamane, Y., Heylbroeck, C., Genin, P., Algarte, M., Servant, M.J., LePage, C., DeLuca, C., Kwon, H., Lin, R., and Hiscott, J. (1999). Interferon regulatory factors: the next generation. Gene *237*, 1–14.

Marie, I., Durbin, J.E., and Levy, D.E. (1998). Differential viral induction of distinct interferon-α genes by positive feedback through interferon regulatory factor-7. EMBO J. *17*, 6660–6669.

Mossman, K.L., Macgregor, P.F., Rozmus, J.J., Goryachev, A.B.,

Edwards, A.M., and Smiley, J.R. (2001). Herpes simplex virus triggers and then disarms a host antiviral response. J. Virol. *75*, 750–758.

Nakagawa, K., and Yokosawa, H. (2000). Degradation of transcription factor IRF-1 by the ubiquitin-proteasome pathway. The C-terminal region governs the protein stability. Eur. J. Biochem. *267*, 1680–1686.

Pickart, C.M. (2000). Ubiquitin in chains. Trends Biochem. Sci. *25*, 544–548.

Poole, L., Yu, Y.X., Kim, P., Zheng, Q.Z., Pevsner, J., and Hayward, G.S. (2002). Altered patterns of cellular gene expression in dermal microvascular endothelial cells infected with the Kaposi's Sarcoma-associated herpesvirus. J. Virol. *76*, 3395–3420.

Sato, M., Suemori, H., Hata, N., Asagiri, M., Ogasawara, K., Nakao, K., Nakaya, T., Katsuki, M., Noguchi, S., Tanaka, N., and Taniguchi, T. (2000). Distinct and essential roles of transcription factors IRF-3 and IRF-7 in response to viruses for IFN-α/β gene induction. Immunity *13*, 539–548.

Scheffner, M., Huibregtse, J.M., Vierstra, R.D., and Howley, P.M. (1993). The HPV-16 E6 and E6-AP complex functions as a ubiquitin-protein ligase in the ubiquitination of p53. Cell *75*, 495–505.

Sun, R., Lin, S.F., Gradoville, L., Yuan, Y., Zhu, F., and Miller, G. (1998). A viral gene that activates lytic cycle expression of Kaposi's sarcoma-associated herpesvirus. Proc. Natl. Acad. Sci. USA *95*, 10866–10871.

Taniguchi, T., Ogasawara, K., Takaoka, A., and Tanaka, N. (2001). IRF family of transcription factors as regulators of host defense. Annu. Rev. Immunol. *19*, 623–655.

Wang, S.E., Wu, F.Y., Fujimuro, M., Zong, J., Hayward, S.D., and Hayward, G.S. (2003). Role of CCAAT/enhancer binding protein α (C/EBPα) in activation of the Kaposi's sarcoma-associated herpesvirus (KSHV) lytic-cycle replication-associated protein (RAP) promoter in cooperation with the KSHV replication and transcription activator (RTA) and RAP. J. Virol. *77*, 600–623.

Wu, F.Y., Chen, H., Wang, S.E., ApRhys, C.M., Liao, G., Fujimuro, M., Farrell, C.J., Huang, J., Hayward, S.D., and Hayward, G.S. (2003). CCAAT/enhancer binding protein α interacts with ZTA and mediates ZTA-induced p21(CIP-1) accumulation and G(1) cell cycle arrest during the Epstein-Barr virus lytic cycle. J. Virol. *77*, 1481–1500

Yokosawa, N., Yokota, S., Kubota, T., and Fujii, N. (2002). C-terminal region of STAT-1α is not necessary for its ubiquitination and degradation caused by mumps virus V protein. J. Virol. *76*, 12683–12690.

Yoneyama, M., Suhara, W., Fukuhara, Y., Fukuda, M., Nishida, E., and Fujita, T. (1998). Direct triggering of the type I interferon system by virus infection: activation of a transcription factor complex containing IRF-3 and CBP/p300. EMBO J. *17*, 1087–1095.

Zhang, L., and Pagano, J.S. (2002). Structure and function of IRF-7. J. Interferon Cytokine Res. *22*, 95–101.

Zhu, F.X., King, S.M., Smith, E.J., Levy, D.E., and Yuan, Y. (2002). A Kaposi's sarcoma-associated herpesviral protein inhibits virus-mediated induction of type I interferon by blocking IRF-7 phosphorylation and nuclear accumulation. Proc. Natl. Acad. Sci. USA *99*, 5573–5578.

Zhu, H., Cong, J.P., and Shenk, T. (1997). Use of differential display analysis to assess the effect of human cytomegalovirus infection on the accumulation of cellular RNAs: induction of interferon-responsive RNAs. Proc. Natl. Acad. Sci. USA *94*, 13985–13990.

Zimring, J.C., Goodbourn, S., and Offermann, M.K. (1998). Human herpesvirus 8 encodes an interferon regulatory factor (IRF) homolog that represses IRF-1-mediated transcription. J. Virol. *72*, 701–707.